



Published in final edited form as:

*Protein Pept Lett.* 2014 March ; 21(3): 235–246.

## Watching Single Proteins Using Engineered Nanopores

Liviu Movileanu<sup>†,§,||,\*</sup>

<sup>†</sup>Department of Physics, Syracuse University, 201 Physics Bldg., Syracuse, New York 13244-1130, USA

<sup>§</sup>Structural Biology, Biochemistry, and Biophysics Program, Syracuse University, 111 College Place, Syracuse, New York 13244-4100, USA

<sup>||</sup>The Syracuse Biomaterials Institute, Syracuse University, 121 Link Hall, Syracuse, New York 13244, USA

### Abstract

Recent studies in the area of single-molecule detection of proteins with nanopores show a great promise in fundamental science, bionanotechnology and proteomics. In this mini-review, I discuss a comprehensive array of examinations of protein detection and characterization using protein and solid-state nanopores. These investigations demonstrate the power of the single-molecule nanopore measurements to reveal a broad range of functional, structural, biochemical and biophysical features of proteins, such as their backbone flexibility, enzymatic activity, binding affinity as well as their concentration, size and folding state. Engineered nanopores in organic materials and in inorganic membranes coupled with surface modification and protein engineering might provide a new generation of sensing devices for molecular biomedical diagnosis.

### Keywords

Polypeptide translocation; Aptamer; Single-channel electrical recordings; Single-channel kinetics; Chemical modification; Protein engineering; Protein folding

## 1. Background and motivation

A single nanopore in an insulating membrane permits translocation of ions from one side of the membrane to the other. This simple process is ubiquitous in biology and biotechnology. Selective ion protein channels traverse the cellular membranes, enabling ionic asymmetries and gradients that exist between the intracellular and extracellular compartments <sup>1</sup>.

However, the protein channels can be specific for a broad range of analytes, from small molecules to long biopolymers, such as proteins and nucleic acids. Inspired by these elements of membrane biology, single-molecule detection with nanopores implies the ability of measuring a small and continuous current across a single protein or synthetic nanometer-scale hole in a membrane (Fig. 1A). If this hole, also called nanopore, contains an attractive reactive group for a specific analyte, then it is selective for that molecule. In this case,

---

Correspondence/reprint requests: Liviu Movileanu, PhD, Department of Physics, Syracuse University, 201 Physics Building, Syracuse, New York 13244-1130, USA; Phone:315-443-8078; Fax: 315-443-9103; lmovilea@physics.syr.edu.

transient binding interactions of the analyte with the reactive group produces reversible current blockades (Fig. 1B). The frequency and duration of the current blockades are dependent on the concentration of the analyte in the aqueous phase and the strength of the binding interaction, respectively (Fig. 1C). The reactive group can be either native or engineered or chemically modified. This mechanism is at the heart of single-molecule stochastic sensing with nanopores<sup>2,3</sup>. This sort of experiments can be extended even to a situation when a reactive (or binding) site does not exist inside the nanopore. In this case, each distinct analyte produces a unique single-channel electrical signature, whose current fluctuations are dependent on the biophysical properties of the partitioning of the analyte into the nanopore.

Single-molecule explorations using protein nanopores have been initiated about two decades ago. Pioneering work was conducted to obtain an understanding of the effect of water-soluble polymers on the single-channel electrical signature of protein nanopores<sup>4-7</sup>. Later, Bezrukov and Kasianowicz explored the excess single-channel noise generated by the reversible ionization sites within the staphylococcal  $\alpha$ -hemolysin ( $\alpha$ HL) protein nanopore<sup>8</sup>, permitting determinations of their kinetic rate constants of association and dissociation<sup>9</sup>. The landmark work of the early days of the nanopore field has been published by the team formed by John Kasianowicz, Eric Brandin, Daniel Branton and David Deamer<sup>10</sup>, who demonstrated that individual single-stranded polynucleotides can pass through a single  $\alpha$ HL protein nanopore reconstituted into a planar lipid bilayer from one side of the bilayer to the other. This translocation of single-stranded polynucleotides, one at a time, occurred as a result of an electric force applied on the translocating polynucleotide owing to an applied transmembrane potential. The outcome of this pioneering work represented, for about 15 years, a platform for a stimulating discovery concept: single-molecule nucleic acid (DNA) sequencing in a linear fashion when a single-stranded DNA can be read, nucleotide by nucleotide, while it traverses a small orifice located into an insulated membrane. Significant progress in understanding DNA passage through nanopores prompted various proposed conceptual schemes for its single-molecule sequencing<sup>11-13</sup>.

However, the single-molecule examinations with nanopores demonstrated the ability to probe a broad range of small molecules and other biopolymers in a way that differed from those studies accomplished in bulk aqueous phase that masked individual dynamic features of molecules under investigation. This idea coupled with additional chemical modification and protein engineering culminated with the proposal of single-molecule stochastic sensing<sup>2,3,14-17</sup>. The underlying mechanism of this concept is the engineering a chemical and functional group at a desired location within a protein nanopore<sup>15,16,18,19</sup>. The reversible interactions of the analyte molecules with the engineered functional (e.g., chemical recognition) group would produce well-defined alterations in the single-channel current measured in the electrical recordings, allowing the direct determinations of the kinetic rate constants of association and dissociation. In this way, stochastic sensing with nanopores has a tremendous advantage for simultaneous detection of the concentration as well as identity of the analyte.

In this mini-review, I will focus my discussion on the achievements in this area pertinent to single-molecule detection and exploration of individual short polypeptides and proteins.

Here, I want to emphasize clear distinctions between nucleic acids and proteins that make the work with the latter more challenging. Single-stranded or double-stranded DNA is a linearized and uniformly charged molecule, carrying one negative charge per each phosphate group. In addition, DNA is a chemically stable polymer, permitting its exploration under harsh conditions of experimentation. These are rather advantages for driving a piece of DNA through a nanopore in a linear fashion, owing to uniform driving force applied on the DNA molecule during its translocation. On the other hand, polypeptides and proteins are not uniformly charged, with distinct parts that are either hydrophilic or hydrophobic, thus forming different folds. Various shapes of proteins, away from linear folds as well as non-uniform distribution of charges along the polypeptide chain, show rather disadvantageous traits for their exploration using nanopores. For example, there is a substantial energetic barrier for a folded protein to partition into a nanopore for the simple reason of the numerous intra-molecular interactions that prevent its immediate unfolding followed by its translocation in a linear fashion.

## 2. Probing polypeptide size, shape and charge

The pioneering work in the area of exploration of polypeptides with nanopores was characterized by a focus on how these polymers partition into the nanopore interior, interact with the protein walls and alter the single-channel electrical parameters of the nanopore, such as ion selectivity and unitary conductance<sup>20–28</sup>. It was an expectation that the modifications of these parameters are strongly dependent on biophysical properties of the polypeptide analytes, including polypeptide size, charge, shape, conformation as well as its dynamic time-dependent folding state. For example, Sanchez-Quesada and colleagues (2000) examined the interactions of four cyclic peptides, *cyclo*[(L-Arg-D-Leu)<sub>4</sub>], *cyclo*[(L-Glu-D-Leu)<sub>4</sub>], *cyclo*-[(-L-Phe-D-N-(aminoethyl)-Ala-L-Phe-D-Ala)<sub>2</sub>] and *cyclo*[(L-Phe-D-N-(carboxymethyl)-Ala-L-Phe-D-Ala)<sub>2</sub>], with the interior of the  $\alpha$ HL protein nanopore<sup>29</sup>. These cyclic peptides were lodged within the nanopore lumen for long periods and served as molecular adapters for a variety of small-molecule analytes, including the second messenger IP<sub>3</sub>. For example, positively charged cyclic peptides were also used as binding site adaptors for a range of polyanions. Later, several groups studied the modulation of the unitary conductance of the  $\alpha$ HL protein nanopore by structured polypeptides.

First, Sutherlands and colleagues (2005) investigated the discrimination of (Gly-Pro-Pro)-containing polypeptide repeats based upon the transit times and the current amplitudes (Fig. 2)<sup>30</sup>. These polypeptides form mixtures of single, double, or collagen-like triple helices. Later, Movileanu and coworkers (2005)<sup>31</sup> and, independently, Stefureac and colleagues (2006)<sup>32</sup>, performed methodical single-channel analyses of the interactions of  $\alpha$ -helical polypeptides with protein nanopores. These interactions are voltage dependent owing to the localized charges on the translocating polypeptide chains. For example, a single-channel study employed (AAKAA)<sub>n</sub>-containing polypeptides interacting with the interior of the  $\alpha$ HL protein nanopore<sup>31</sup>. Because the repetitive unit has a single positive charge, this polypeptide series has molecules whose length is linearly increasing their charge. The kinetic rate constants of association, given by  $1/c \tau_{on}$ , where  $c$  is the polypeptide concentration and  $\tau_{on}$  is the inter-event time interval, increased exponentially with increasing applied transmembrane potential. In contrast, the dissociation constants underwent a U-shape profile with the

applied transmembrane potential. This finding indicated two kinetic regimes by varying the applied transmembrane potential<sup>33</sup>. At lower voltages, the binding of polypeptides to the nanopore interior was dominant, with a small probability of translocation for one side of the bilayer to the other. On the contrary, at higher transmembrane potentials, the free energy contribution associated with the electrical pulling force on the polypeptide dominates, producing a drastic increase in the probability of translocation. The presence of these two regimes in the kinetic rate constant of association and dissociation was also found in a polypeptide translocation study in which electrostatic traps were engineered at the entry and exit of the  $\beta$  barrel of the  $\alpha$ HL protein nanopore<sup>34–36</sup>. However, different size and folding characteristics of the interacting polypeptide might result in deviations from this two-regime kinetic behavior<sup>37</sup>. For instance, for a short beta-hairpin peptide, the rate constant of dissociation increases exponentially with elevated voltages, suggesting that the free energy landscape for the peptide-nanopore interaction has a single barrier and the events represent individual translocations of the peptides from one side of the bilayer to the other<sup>38</sup>. On the other hand, large and folded proteins are not supposed to translocate across the nanopores under native experimental conditions of ionic strength and pH<sup>39–42</sup>.

### 3. Monitoring protein folding and unfolding with nanopores

A folded protein, whose dimensions are greater than the internal diameter of a nanopore cannot traverse it from one side of the membrane to the other. Therefore, the protein must unfold first, either completely or gradually, in a linear fashion while crossing the nanopore. This is, in fact, a ubiquitous process in molecular biology of the cell<sup>43–46</sup>, and it was extensively examined using theoretical biophysics and computational approaches by Andricioaei's<sup>47</sup>, Kolomeisky's<sup>48, 49</sup>, Muthukumar's<sup>33, 50</sup> and Makarov's<sup>38, 51–55</sup> groups. Based on these arguments, nanopores can serve as a versatile single-molecule probe for protein folding and unfolding<sup>15, 18</sup>. In 2006, Jung and colleagues studied the current fluctuations produced by a small elastin-like polypeptide (ELP) loop engineered within the large vestibule of the  $\alpha$ HL protein nanopore<sup>56</sup> (Fig. 3A). It is well known that ELPs undergo inverse transition temperatures ( $T_i$ ), meaning that they are well-hydrated and unfolded at temperatures lower than  $T_i$ , but dehydrated and structurally collapsed at temperatures greater than  $T_i$ <sup>57–59</sup>.

This behavior has been attributed to the fragility of the water layer around the polypeptide bond owing to many hydrophobic residues present within the ELP sequence. Therefore, an ELP shrinks at temperatures above the transition temperature and expands at temperatures below the transition temperature. Indeed, single-channel electrical recordings with ELP-containing  $\alpha$ HL produced current blockades, whose residual current was temperature dependent. This finding suggested that the overall size of ELP occluding the narrower  $\beta$ -barrel domain was dependent on the absolute temperature in the chamber. Thus, at a temperature of 20°C, well below the transition temperature of ~39°C, a 50-residue long ELP produced full single-channel current blockades (Fig. 3B). Interestingly, if the temperature in the chamber approached  $T_i$ , then a residual current of the current blockades was observed (Fig. 3C), which was apparent at 60°C, well above  $T_i$  (Fig. 3D). These results were interpreted in terms of the temperature-dependent structural alterations of the engineered ELP loop. Below its  $T_i$ , the ELP loop was fully expanded, well-hydrated and occluded

completely, but reversibly, the ion permeation pathway across the  $\alpha$ HL protein nanopore. In contrast, at a temperature greater than  $T_i$ , the ELP backbone underwent a dehydration process, whereas its structure collapsed, permitting an ion flow across the nanopore. This process resulted in an increased residual current as compared to the values observed at lower temperatures. The design of these experiments can also be expanded to future studies targeting the single-molecule observation of protein folding and unfolding under confinement circumstances. Moreover, design of loop-containing protein nanopores, in which various sequences and location of the engineered polypeptide are employed, might also provide a better understanding of the mechanisms underlying the stochastic current fluctuations observed with  $\beta$ -barrel proteins<sup>60–67</sup>.

I mentioned above that protein translocation across a single protein nanopore in a membrane is closely related to its unfolding process in order to make the protein “translocation competent”<sup>43, 68, 69</sup>. This nanopore-mediated unfolding problem was explored extensively by Loic Auvray’s team<sup>33, 70–74</sup>. Their experiments were inspired by the lessons learned from the realm of protein folding in the last couple of decades. Pioneered work in this area culminated with a landmark study, in which the translocation of the maltose binding protein (MBP), a 370-residue long polypeptide (~40.7 kDa), interacted with the  $\alpha$ HL protein nanopore in a fashion depending on its unfolding state<sup>70</sup>. The protein unfolding was induced by the chemical denaturant guanidinium hydrochloride (Gdm-HCl). By varying the concentration of Gdm-HCl in the chamber, the unfolding state of the interacting protein was correlated with the frequency and duration of the MBP-induced, single-channel current blockades. It was found that the duration of very short-lived current blockades increased upon the denaturation of MBP. The single-channel data analysis also indicated long-lived MBP-induced current blockades, which were attributed to the presence of the partly folded MBP in the chamber. Later, these studies were naturally expanded by using temperature as a denaturing stimulus<sup>74</sup>. The thermally induced unfolding of MBP, coupled with its interaction with either the  $\alpha$ HL protein nanopore or the aerolysin protein nanopore, was examined extensively in the range 10–70°C, revealing an important characteristic of nanopore systems: their stability over a broad temperature range owing to the rigidity of the  $\beta$ -barrel scaffolds. It is worth mentioning that the transition temperature found by Payet and colleagues (2012) was not dependent on the nanopore employed in this work<sup>74</sup>. The validity of these systematical single-channel studies was further confirmed by employing a mutant of MBP (MalE219), which is partly destabilized under physiological conditions<sup>71, 73</sup>. Indeed, the transition temperature of the less stable, interacting protein occurred at a lower temperature value than in the case of the wild-type MBP.

One point I want to emphasize here is the distinction between two different processes: thermodynamic (or global) unfolding and mechanical unfolding<sup>54</sup>. The thermodynamic or global unfolding of proteins is mediated either by temperature or by chemical denaturants. The mechanical unfolding is facilitated by the pulling force acting on the charged sites of the protein. These two processes undergo different free energy landscapes. Therefore, both kinetics and thermodynamics of nanopore-mediated protein unfolding and protein denaturation via temperature jump or the presence of chemical denaturants, such as urea and Gdm-HCl, and mechanical unfolding are expected to be different. This is the primary reason

why the protein unfolding mediated by the mitochondrial protein nanopores and achieved by the active ATP-dependent motor proteins (such as Hsp70) occurs with a much faster rate, about two orders of magnitude, than the corresponding global (or thermodynamic) unfolding rates measured in vitro by the presence of chemical denaturants<sup>75, 76</sup>. The kinetic rate constants of association and dissociation of polypeptide translocation through protein and synthetic nanopores cover a broad range owing to the large variability in the polypeptide charge, folding state and backbone flexibility for native and engineered systems<sup>31, 38, 45, 46</sup>. Moreover, the effective charge of the polypeptide within a single nanopore strongly depends on the salt concentration<sup>33, 77</sup>. Other important factors, which are usually ignored, include the geometry, size and surface charge of the nanopores. The overall impact of these parameters on the magnitude of the kinetic rate constants is also reflected on the effective force acting on an unfolded polypeptide translocating across a single nanopore in a membrane. In addition, these experimental circumstances influence the free energy landscape as well as the corresponding heights of the activation free energies. In general, the effective force on a short unfolded polypeptide chain within a protein nanopore is several pN<sup>38, 78</sup>. The activation free energy for the partitioning of a polypeptide into a single nanopore is in the range of 2 through 12  $k_B T$ <sup>31, 70-72</sup>. However, it is an expectation that the energetic barriers are greater in native protein translocation systems. Therefore, ATP-dependent active forces produced the molecular motors are employed to overcome these thermodynamic penalties<sup>79, 80</sup>.

In the last few years, protein translocation and unfolding was aggressively investigated using solid-state nanopores<sup>33, 78, 81-93</sup>. Han and coworkers (2006) used solid-state nanopores to examine proteins<sup>82</sup>. One year later, Fologea and colleagues (2007) employed synthetic nanopores to study the translocation of bovine serum albumin (BSA)<sup>83</sup>. Using a chemiluminescence assay, they were able to provide evidence of full translocation of BSA from one side of the membrane to the other. Moreover, by varying pH in the chamber, they determined the charge state of the protein. Li and Talaga (2009)<sup>78</sup> and Freedman and colleagues (2011)<sup>90</sup> investigated the protein unfolding using a solid-state nanopore as a single-molecule probe and correlated their findings with the excluded volume of single proteins adopting various conformations.

One drawback of the silicon nitride surface is its susceptibility to nonspecific adsorption of polypeptides of varying amino acid sequence, size and conformation<sup>86, 87</sup>. This technical limitation has recently been addressed by functionalization of the silicon nitride membrane surface with a fluid lipid bilayer. Yusko and colleagues (2011) were able to prevent nonspecific adsorption of proteins by coating the surface of the nanopore with a biomolecule compatible and versatile lipid bilayer, which permitted insertion of chemical ligands for capturing targeted protein analytes<sup>91</sup> (Fig. 4A). This is a very innovative approach that demonstrates a first breakthrough step for expanding the single-molecule nanopore measurements in the area of protein detection. In the absence of chemically modified lipids with biotin groups, rare and short-lived events were observed. In contrast, the presence of biotin-containing lipids increased the frequency and duration of binding protein-produced current blockades. With future critical developments, this experimental design has promise in protein detection assays by concentrating proteins from diluted solutions and probing

time-resolvable kinetic rates, providing useful information of binding affinity of the ligands to the targeted proteins. Conceptually, there is no technical difficulty in replacing the biotin ligand with other attractive chemical group of different dimensions and there is not challenge in altering the binding protein. To offer a proof of principle for protein adsorption-free current recordings, probing individual aggregates of amyloid-beta (A $\beta$ ) peptide was conducted for tens of minutes with a lipid bilayer-coated, solid-state nanopore, which otherwise was unachievable with an uncoated silicon nitride nanopore (Fig. 4B and Fig. 4C).

#### 4. Monitoring enzymatic activities of proteins

In the previous sections of this mini-review, we discussed applications of nanopores in probing proteins based on their size, shape, charge and folding state. Here, we identify that nanopores can also be employed to probe enzymatic activities of proteins. A stochastic sensor element for probing enzymatic reactions was first designed by Xie and collaborators (2005)<sup>94, 95</sup>. In this case, a peptide inhibitor was directly engineered into the polypeptide chain of the  $\alpha$ HL protein nanopore, near one of its entrances. A detailed kinetic and thermodynamic analysis of the interactions between the catalytic subunit of the cAMP-dependent protein kinase A (PKA) with the engineered peptide inhibitor was derived from the individual stochastic current blockades. In this way, engineered protein nanopores might be used in the future for selective nanostructures employed for rapid screening of enzymatic inhibitors. More recently, engineered protein nanopores were employed in monitoring the protease activity of various enzymes<sup>96–99</sup>.

#### 5. Probing proteins via protein-ligand interactions

Exploring proteins with nanopore-based approaches by employing their interactions with other ligands has been a very active area in the last decade or so. Single-molecule protein detection was first accomplished via a ligand tethered on a movable polymeric arm that was covalently attached within the interior of the  $\alpha$ HL protein nanopore<sup>100, 101</sup>. Later, Howorka and colleagues (2004)<sup>102</sup> and Rotem and coworkers (2012)<sup>103</sup> naturally expanded this molecular design to other applications. In the former application, multivalent interactions were probed at the single-molecule level via the binding kinetics of a lectin protein to one or more ligands via a linker covalently attached to the interior of the  $\alpha$ HL protein nanopore. The attachment site was an engineered Cys residue near the entrance of the  $\alpha$ HL protein nanopore<sup>17, 103, 104</sup>. In the latter application, proteins were captured from the chamber via their corresponding targeted aptamers covalently attached to a similar position. These are just a few examples that illustrate the unquestionable power of protein nanopores to accommodate engineered or chemically modified functional groups at strategic positions within the nanopore interior and with an atomic precision. In the last few years, protein nanopore-based sensors were designed by coating the solid-state nanopore walls with various ligands. One example was the biofunctionalization of a conical gold nanotube sensor with a molecular recognition group<sup>81, 84, 89</sup>. It is worth mentioning that this was not a single-molecule protein detection measurement, because the current recordings were not deemed to detect individual protein binding events. Overall, pioneering work in protein detection using nanopores used small ligand-protein<sup>101, 102, 105</sup>, but also peptide-protein<sup>94, 95</sup>, and antibody-protein interactions<sup>81, 84, 85, 89</sup>. In the very recent years,

investigators realized the opportunity of inspecting either proteins or nucleic acids by using their native interactions<sup>12, 13, 106–116</sup>. This was further expanded towards single-molecule nanopore-based protein detection using DNA and RNA aptamers<sup>99, 103, 117–120</sup>.

A landmark piece of work in the area of single-molecule detection of proteins with nanopores is the study performed very recently by Wei and coworkers (2012)<sup>92</sup>, who were able to monitor individual single-molecule bindings of proteins with targeted ligands placed on the nanopore walls (Fig. 5). A single metallized nanopore was chemically functionalized with a single monolayer of alkane thiols, polyethylene glycol (PEG) thiols as well as multivalent nitriloacetic (NTA) thiols. Such a surface chemistry design permitted the attachment of hexahistidine (His<sup>6+</sup>)-tagged protein A, which served as a secondary protein for binding to anti-protein A polypeptides, such as IgG derivatives. In this way, Wei and colleagues have generated an antibody-selective nanopore. Individual binding events of IgG protein derivatives and protein A produced single-channel current blockades, whose kinetics and thermodynamics were strongly dependent on the position of the reactive protein A. Voltage-dependence single-channel data analysis also identified that the kinetic dissociation constant strongly depended on the position of the receptor position. Moreover, it was shown that the binding affinity was a function depending on the multivalence of the receptor protein. Overall, this study shows a great promise for employing functionalized solid-state nanopores in proteomic analysis.

## 6. Comparisons with other single-molecule approaches for examining proteins and their complexes with different molecules

The single-molecule analysis of short polypeptides and proteins can also be pursued by other techniques, such as single-molecule force spectroscopy<sup>121, 122</sup>, which includes atomic force microscopy (AFM)<sup>121, 123, 124</sup>, nanopore force spectroscopy<sup>107, 125, 126</sup> and optical tweezers<sup>123, 127</sup>. Moreover, significant progress has been accomplished in the area of single-molecule fluorescence microscopy<sup>128</sup> of proteins and their ensembles with other proteins and nucleic acids, such as single-molecule fluorescence resonance energy transfer (FRET)<sup>129–135</sup>. The AFM techniques are employed either in the imaging mode for nanoscale visualization of proteins and their complexes with other proteins or nucleic acids, or in the force spectroscopy mode for determining force-extension curves on multidomain proteins. The force-extension curves probe the force strength associated with the folding of multiple protein domains. Each domain corresponds to a load drop in the force-extension curve. Mechanical unfolding of proteins can also be pursued by using optical tweezers. In this case, one terminal of the protein is attached to a horizontal stage, whereas the other terminal is covalently linked to an optically controlled microbead. Importantly, the optical tweezer features resolvability of forces of at least one order of magnitude smaller than those probed by AFM, namely in the range of a few pN. The lower force resolution in the case of AFM is mainly caused by the large elastic constant of the cantilever. In nanopore force spectroscopy, a nucleic acid, which is bound to a protein, is driven across a nanopore using a feedback mechanism on the applied transmembrane potential. This approach enables the determination of the energy barriers required to overcome for the dissociation of a nucleic acid from a binding protein. This approach can also be expanded to the examination of

mechanical unfolding of single polypeptides. However, one difficulty for data interpretation resides in the nonuniformity of the charge distribution along the polypeptide chain, producing the nonuniformity of the applied electrical force on the polypeptide. It is worth mentioning that the mechanical unfolding of a single protein via AFM or an optical tweezer undergoes a distinct energetic landscape from that corresponding to mechanical unfolding via nanopore force spectroscopy owing to the excluded volume arguments<sup>55</sup>. In contrast to these approaches, the dynamics of folding-unfolding of a single protein using single-molecule FRET techniques requires labeling of the protein under investigation using two fluorophores. The underlying mechanism for signal detection relies on a distance-dependent energy transfer between a donor and an acceptor. This process implies supplementary chemical modifications or protein engineering, which might alter the transient dynamics of various kinetic substates of the protein. Moreover, changes of the experimental circumstances, such as temperature, osmotic agents and pH, might induce further modifications in the optical stability of the fluorophores. In contrast, such a labeling for the real-time detection of the dynamics of a protein is not a requirement in single-molecule nanopore technology. Finally, all techniques described in this section do not show promise for parallelization and high-throughput assays, a feature that can be advantageously employed with single-molecule probe techniques.

## 7. Future prospects

In this mini-review, I briefly discussed an array of single-molecule studies employing nanopores for the detection and characterization of individual proteins. These studies illustrate the power of the single-molecule, nanopore technologies for discriminating proteins and for examining their biochemical and biophysical features. There are still numerous problems to be addressed. One important issue in protein folding is the clarification of the mechanisms driving progressive protein unfolding within a nanopore. This is a ubiquitous process in the biology of protein translocation and protein degradation. Unraveling of a protein in a linear fashion might be tackled by a combination of force measurements with electrical recordings. Such measurements have been already accomplished with a single piece of single-stranded DNA threaded across a single solid-state nanopore and controlled by an optical trap<sup>136, 137</sup>. Another issue is still controlling a receptor attachment within a solid-state nanopore at a desired position with an atomic precision. While this can be routinely accomplished with a protein nanopore<sup>3</sup>, it seems hard to get it accomplished with a solid-state nanopore. An alternative solution is obtaining a hybrid device that integrates a robust protein nanopore with a solid-state nanopore. This was recently achieved by electrophoretic driving an  $\alpha$ HL protein nanopore into a silicon nitride-based nanopore<sup>138</sup>. Finally, other issues have to be addressed in regard to selective screening schemes for protein-based biomarkers, including high time-resolution electrical measurements for detecting low binding affinity of proteins<sup>139</sup>.

## Acknowledgments

I apologize to all those who cannot see their work cited in this mini-review, either due to my ignorance or the limits and focus of this article. I am deeply grateful to all colleagues in my research group. This paper was funded in part by grants from the US National Science Foundation (DMR-1006332) and the National Institutes of Health (R01 GM088403).

## Reference List

1. Hille, B. *Ion Channels of Excitable Membranes*. Sunderland, Massachusetts, USA: Sinauer Associates, Inc; 2001.
2. Bayley H, Martin CR. Resistive-pulse sensing - From microbes to molecules. *Chem Rev*. 2000; 100:2575–2594. [PubMed: 11749296]
3. Bayley H, Cremer PS. Stochastic sensors inspired by biology. *Nature*. 2001; 413:226–230. [PubMed: 11557992]
4. Zimmerberg J, Parsegian VA. Polymer inaccessible volume changes during opening and closing of a voltage-dependent ionic channel. *Nature*. 1986; 323:36–39. [PubMed: 2427958]
5. Vodyanoy I, Bezrukov SM. Sizing of an ion pore by access resistance measurements. *Biophys J*. 1992; 62:10–11. [PubMed: 1376161]
6. Bezrukov SM, Vodyanoy I. Probing alamethicin channels with water-soluble polymers - Effect on conductance of channel states. *Biophys J*. 1993; 64:16–25. [PubMed: 7679295]
7. Vodyanoy I, Bezrukov SM, Parsegian VA. Probing alamethicin channels with water-soluble polymers - size-modulated osmotic action. *Biophys J*. 1993; 65:2097–2105. [PubMed: 7507718]
8. Bezrukov SM, Kasianowicz JJ. Current noise reveals protonation kinetics and number of ionizable sites in an open protein ion channel. *Phys Rev Lett*. 1993; 70:2352–2355. [PubMed: 10053539]
9. Kasianowicz JJ, Bezrukov SM. Protonation dynamics of the alpha-toxin ion-channel from spectral-analysis of pH-dependent current fluctuations. *Biophys J*. 1995; 69:94–105. [PubMed: 7545444]
10. Kasianowicz JJ, Brandin E, Branton D, Deamer DW. Characterization of individual polynucleotide molecules using a membrane channel. *Proc Natl Acad Sci U S A*. 1996; 93:13770–13773. [PubMed: 8943010]
11. Branton D, Deamer DW, Marziali A, Bayley H, Benner SA, Butler T, Di Ventra M, Garaj S, Hibbs A, Huang X, Jovanovich SB, Krstic PS, Lindsay S, Ling XS, Mastrangelo CH, Meller A, Oliver JS, Pershin YV, Ramsey JM, Riehn R, Soni GV, Tabard-Cossa V, Wanunu M, Wigginton M, Schloss JA. The potential and challenges of nanopore sequencing. *Nat Biotechnol*. 2008; 26:1146–1153. [PubMed: 18846088]
12. Cherf GM, Lieberman KR, Rashid H, Lam CE, Karplus K, Akeson M. Automated forward and reverse ratcheting of DNA in a nanopore at 5-A precision. *Nat Biotechnol*. 2012; 30:344–348. [PubMed: 22334048]
13. Manrao EA, Derrington IM, Laszlo AH, Langford KW, Hopper MK, Gillgren N, Pavlenok M, Niederweis M, Gundlach JH. Reading DNA at single-nucleotide resolution with a mutant MspA nanopore and phi29 DNA polymerase. *Nat Biotechnol*. 2012; 30:349–353. [PubMed: 22446694]
14. Bayley H, Braha O, Gu LQ. Stochastic sensing with protein pores. *Adv Mater*. 2000; 12:139–142.
15. Movileanu L. Interrogating single proteins through nanopores: challenges and opportunities. *Trends Biotechnol*. 2009; 27:333–341. [PubMed: 19394097]
16. Majd S, Yusko EC, Billeh YN, Macrae MX, Yang J, Mayer M. Applications of biological pores in nanomedicine, sensing, and nanoelectronics. *Curr Opin Biotechnol*. 2010; 21:439–476. [PubMed: 20561776]
17. Howorka S, Siwy ZS. Nanopores as protein sensors. *Nat Biotechnol*. 2012; 30:506–507. [PubMed: 22678388]
18. Movileanu L. Squeezing a single polypeptide through a nanopore. *Soft Matter*. 2008; 4:925–931.
19. Howorka S, Siwy Z. Nanopore analytics: sensing of single molecules. *Chem Soc Rev*. 2009; 38:2360–2384. [PubMed: 19623355]
20. Henry JP, Chich JF, Goldschmidt D, Thieffry M. Blockade of a mitochondrial cationic channel by an addressing peptide: an electrophysiological study. *J Membr Biol*. 1989; 112:139–147. [PubMed: 2482895]
21. Henry JP, Chich JF, Goldschmidt D, Thieffry M. Ionic mitochondrial channels: characteristics and possible role in protein translocation. *Biochimie*. 1989; 71:963–968. [PubMed: 2478198]
22. Thieffry M, Neyton J, Pelleschi M, Fevre F, Henry JP. Properties of the mitochondrial peptide-sensitive cationic channel studied in planar bilayers and patches of giant liposomes. *Biophys J*. 1992; 63:333–339. [PubMed: 1384736]

23. Henry JP, Juin P, Vallette F, Thieffry M. Characterization and function of the mitochondrial outer membrane peptide-sensitive channel. *J Bioenerg Biomembr.* 1996; 28:101–108. [PubMed: 9132407]
24. Juin P, Thieffry M, Henry JP, Vallette FM. Relationship between the peptide-sensitive channel and the mitochondrial outer membrane protein translocation machinery. *J Biol Chem.* 1997; 272:6044–6050. [PubMed: 9038228]
25. Hinnah SC, Hill K, Wagner R, Schlicher T, Soll J. Reconstitution of a chloroplast protein import channel. *EMBO J.* 1997; 16:7351–7360. [PubMed: 9405364]
26. Kunkle KP, Juin P, Pompa C, Nargang FE, Henry JP, Neupert W, Lill R, Thieffry M. The isolated complex of the translocase of the outer membrane of mitochondria. Characterization of the cation-selective and voltage-gated preprotein-conducting pore. *J Biol Chem.* 1998; 273:31032–31039. [PubMed: 9813001]
27. Hinnah SC, Wagner R, Sveshnikova N, Harrer R, Soll J. The chloroplast protein import channel Toc75: Pore properties and interaction with transit peptides. *Biophys J.* 2002; 83:899–911. [PubMed: 12124272]
28. Muro C, Grigoriev SM, Pietkiewicz D, Kinnally KW, Campo ML. Comparison of the TIM and TOM channel activities of the mitochondrial protein import complexes. *Biophys J.* 2003; 84:2981–2989. [PubMed: 12719229]
29. Sanchez-Quesada J, Ghadiri MR, Bayley H, Braha O. Cyclic peptides as molecular adapters for a pore-forming protein. *J Am Chem Soc.* 2000; 122:11757–11766.
30. Sutherland TC, Long YT, Stefureac RI, Bediako-Amoa I, Kraatz HB, Lee JS. Structure of peptides investigated by nanopore analysis. *Nano Lett.* 2005; 4:1273–1277.
31. Movileanu L, Schmittschmitt JP, Scholtz JM, Bayley H. Interactions of the peptides with a protein pore. *Biophys J.* 2005; 89:1030–1045. [PubMed: 15923222]
32. Stefureac R, Long YT, Kraatz HB, Howard P, Lee JS. Transport of alpha-Helical Peptides through alpha-Hemolysin and Aerolysin Pores. *Biochemistry.* 2006; 45:9172–9179. [PubMed: 16866363]
33. Cressiot B, Oukhaled A, Patriarche G, Pastoriza-Gallego M, Betton JM, Auvray L, Muthukumar M, Bacri L, Pelta J. Protein Transport through a Narrow Solid-State Nanopore at High Voltage: Experiments and Theory. *ACS Nano.* 2012; 6:6236–6243. [PubMed: 22670559]
34. Wolfe AJ, Mohammad MM, Cheley S, Bayley H, Movileanu L. Catalyzing the translocation of polypeptides through attractive interactions. *J Am Chem Soc.* 2007; 129:14034–14041. [PubMed: 17949000]
35. Mohammad MM, Movileanu L. Excursion of a single polypeptide into a protein pore: simple physics, but complicated biology. *Eur Biophys J.* 2008; 37:913–925. [PubMed: 18368402]
36. Bikwemu R, Wolfe AJ, Xing X, Movileanu L. Facilitated translocation of polypeptides through a single nanopore. *J Phys : Condens Matter.* 2010; 22:454117. [PubMed: 21339604]
37. Zhao Q, Jayawardhana DA, Wang D, Guan X. Study of Peptide Transport through Engineered Protein Channels. *J Phys Chem B.* 2009; 113:3572–3578. [PubMed: 19231820]
38. Goodrich CP, Kirmizialtin S, Huyghues-Despointes BM, Zhu AP, Scholtz JM, Makarov DE, Movileanu L. Single-molecule electrophoresis of beta-hairpin peptides by electrical recordings and Langevin dynamics simulations. *J Phys Chem B.* 2007; 111:3332–3335. [PubMed: 17388500]
39. Mohammad MM, Prakash S, Matouschek A, Movileanu L. Controlling a single protein in a nanopore through electrostatic traps. *J Am Chem Soc.* 2008; 130:4081–4088. [PubMed: 18321107]
40. Stefureac R, Waldner L, Howard P, Lee JS. Nanopore analysis of a small 86-residue protein. *Small.* 2008; 4:59–63. [PubMed: 18058890]
41. Stefureac RI, Lee JS. Nanopore analysis of the folding of zinc fingers. *Small.* 2008; 4:1646–1650. [PubMed: 18819138]
42. Stefureac RI, Madampage CA, Andrievskaia O, Lee JS. Nanopore analysis of the interaction of metal ions with prion proteins and peptides. *Biochem Cell Biol.* 2010; 88:347–358. [PubMed: 20453935]
43. Krantz BA, Melnyk RA, Zhang S, Juris SJ, Lacy DB, Wu Z, Finkelstein A, Collier RJ. A phenylalanine clamp catalyzes protein translocation through the anthrax toxin pore. *Science.* 2005; 309:777–781. [PubMed: 16051798]

44. Wickner W, Schekman R. Protein translocation across biological membranes. *Science*. 2005; 310:1452–1456. [PubMed: 16322447]
45. Romero-Ruiz M, Mahendran KR, Eckert R, Winterhalter M, Nussberger S. Interactions of mitochondrial presequence peptides with the mitochondrial outer membrane preprotein translocase TOM. *Biophys J*. 2010; 99:774–781. [PubMed: 20682254]
46. Mahendran KR, Romero-Ruiz M, Schlosinger A, Winterhalter M, Nussberger S. Protein translocation through Tom40: kinetics of peptide release. *Biophys J*. 2012; 102:39–47. [PubMed: 22225796]
47. Tian P, Andricioaei I. Repetitive pulling catalyzes co-translocational unfolding of barnase during import through a mitochondrial pore. *J Mol Biol*. 2005; 350:1017–1034. [PubMed: 15979642]
48. Slonkina E, Kolomeisky AB. Polymer translocation through a long nanopore. *J Chem Phys*. 2003; 118:7112–7118.
49. Kolomeisky AB. Channel-facilitated molecular transport across membranes: attraction, repulsion, and asymmetry. *Phys Rev Lett*. 2007; 98:048105. [PubMed: 17358819]
50. Kong CY, Muthukumar M. Simulations of stochastic sensing of proteins. *J Am Chem Soc*. 2005; 127:18252–18261. [PubMed: 16366579]
51. Huang L, Kirmizialtin S, Makarov DE. Computer simulations of the translocation and unfolding of a protein pulled mechanically through a pore. *J Chem Phys*. 2005; 123:124903. [PubMed: 16392523]
52. Huang L, Makarov DE. Translocation of a knotted polypeptide through a pore. *J Chem Phys*. 2008; 129:121107. [PubMed: 19044999]
53. Kirmizialtin S, Ganesan V, Makarov DE. Translocation of a beta-hairpin-forming peptide through a cylindrical tunnel. *J Chem Phys*. 2004; 121:10268–10277. [PubMed: 15549903]
54. Kirmizialtin S, Huang L, Makarov DE. Computer simulations of protein translocation. *Phys Stat Sol (b)*. 2006; 243:2038–2047.
55. Makarov DE. Computer simulations and theory of protein translocation. *Acc Chem Res*. 2008; 42:281–289. [PubMed: 19072704]
56. Jung Y, Bayley H, Movileanu L. Temperature-responsive protein pores. *J Am Chem Soc*. 2006; 128:15332–15340. [PubMed: 17117886]
57. Yamaoka T, Tamura T, Seto Y, Tada T, Kunugi S, Tirrell DA. Mechanism for the phase transition of a genetically engineered elastin model peptide (VPGIG)(40) in aqueous solution. *Biomacromolecules*. 2003; 4:1680–1685. [PubMed: 14606895]
58. Meyer DE, Chilkoti A. Quantification of the effects of chain length and concentration on the thermal behavior of elastin-like polypeptides. *Biomacromolecules*. 2004; 5:846–851. [PubMed: 15132671]
59. Zhang Y, Trabbic-Carlson K, Albertorio F, Chilkoti A, Cremer PS. Aqueous two-phase system formation kinetics for elastin-like polypeptides of varying chain length. *Biomacromolecules*. 2006; 7:2192–2199. [PubMed: 16827587]
60. Biswas S, Mohammad MM, Patel DR, Movileanu L, van den Berg B. Structural insight into OprD substrate specificity. *Nat Struct Mol Biol*. 2007; 14:1108–1109. [PubMed: 17952093]
61. Biswas S, Mohammad MM, Movileanu L, van den Berg B. Crystal structure of the outer membrane protein OpdK from *Pseudomonas aeruginosa*. *Structure*. 2008; 16:1027–1035. [PubMed: 18611376]
62. Mohammad MM, Movileanu L. Impact of distant charge reversals within a robust beta-barrel protein pore. *J Phys Chem B*. 2010; 114:8750–8759. [PubMed: 20540583]
63. Cheneke BR, van den Berg B, Movileanu L. Analysis of gating transitions among the three major open states of the OpdK channel. *Biochemistry*. 2011; 50:4987–4997. [PubMed: 21548584]
64. Liu J, Eren E, Vijayaraghavan J, Cheneke BR, Indic M, van den Berg B, Movileanu L. OccK Channels from *Pseudomonas aeruginosa* Exhibit Diverse Single-channel Electrical Signatures, but Conserved Anion Selectivity. *Biochemistry*. 2012; 51:2319–2330. [PubMed: 22369314]
65. Liu J, Wolfe AJ, Eren E, Vijayaraghavan J, Indic M, van den Berg B, Movileanu L. Cation Selectivity is a Conserved Feature in the OccD Subfamily of *Pseudomonas aeruginosa*. *Biochim Biophys Acta - Biomembr*. 2012; 1818:2908–2916.

66. Cheneke BR, Indic M, van den Berg B, Movileanu L. An Outer Membrane Protein undergoes Enthalpy- and Entropy-driven Transitions. *Biochemistry*. 2012; 51:5348–5358. [PubMed: 22680931]
67. Eren E, Vijayaraghavan J, Liu J, Cheneke BR, Touw DS, Lepore BW, Indic M, Movileanu L, van den Berg B. Substrate specificity within a family of outer membrane carboxylate channels. *PLoS Biology*. 2012; 10:e1001242. [PubMed: 22272184]
68. Krantz BA, Trivedi AD, Cunningham K, Christensen KA, Collier RJ. Acid-induced unfolding of the amino-terminal domains of the lethal and edema factors of anthrax toxin. *J Mol Biol*. 2004; 344:739–756. [PubMed: 15533442]
69. Krantz BA, Finkelstein A, Collier RJ. Protein Translocation through the Anthrax Toxin Transmembrane Pore is Driven by a Proton Gradient. *J Mol Biol*. 2006; 355:968–979. [PubMed: 16343527]
70. Oukhaled G, Mathe J, Biance AL, Bacri L, Betton JM, Lairez D, Pelta J, Auvray L. Unfolding of proteins and long transient conformations detected by single nanopore recording. *Phys Rev Lett*. 2007; 98:158101. [PubMed: 17501386]
71. Pastoriza-Gallego M, Rabah L, Gibrat G, Thiebot B, van der Goot FG, Auvray L, Betton JM, Pelta J. Dynamics of Unfolded Protein Transport through an Aerolysin Pore. *J Am Chem Soc*. 2011; 133:2923–2931. [PubMed: 21319816]
72. Oukhaled A, Cressiot B, Bacri L, Pastoriza-Gallego M, Betton JM, Bourhis E, Jede R, Gierak J, Auvray L, Pelta J. Dynamics of Completely Unfolded and Native Proteins through Solid-State Nanopores as a Function of Electric Driving Force. *ACS Nano*. 2011; 5:3628–3638. [PubMed: 21476590]
73. Merstorf C, Cressiot B, Pastoriza-Gallego M, Oukhaled A, Betton JM, Auvray L, Pelta J. Wild type, mutant protein unfolding and phase transition detected by single-nanopore recording. *ACS Chem Biol*. 2012; 7:652–658. [PubMed: 22260417]
74. Payet L, Martinho M, Pastoriza-Gallego M, Betton JM, Auvray L, Pelta J, Mathe J. Thermal unfolding of proteins probed at the single molecule level using nanopores. *Anal Chem*. 2012; 84:4071–4076. [PubMed: 22486207]
75. Matouschek A. Protein unfolding--an important process in vivo? *Curr Opin Struct Biol*. 2003; 13:98–109. [PubMed: 12581666]
76. Prakash S, Matouschek A. Protein unfolding in the cell. *Trends Biochem Sci*. 2004; 29:593–600. [PubMed: 15501678]
77. Sauer-Budge AF, Nyamwanda JA, Lubensky DK, Branton D. Unzipping kinetics of double-stranded DNA in a nanopore. *Phys Rev Lett*. 2003; 90:art-238101.
78. Talaga DS, Li J. Single-molecule protein unfolding in solid state nanopores. *J Am Chem Soc*. 2009; 131:9287–9297. [PubMed: 19530678]
79. Huang S, Ratliff KS, Schwartz MP, Spenner JM, Matouschek A. Mitochondria unfold precursor proteins by unraveling them from their N-termini. *Nat Struct Biol*. 1999; 6:1132–1138. [PubMed: 10581555]
80. Huang S, Ratliff KS, Matouschek A. Protein unfolding by the mitochondrial membrane potential. *Nat Struct Biol*. 2002; 9:301–307. [PubMed: 11887183]
81. Siwy Z, Trofin L, Kohli P, Baker LA, Trautmann C, Martin CR. Protein biosensors based on biofunctionalized conical gold nanotubes. *J Am Chem Soc*. 2005; 127:5000–5001. [PubMed: 15810817]
82. Han A, Schurmann G, Monding G, Bitterli RA, de Rooij NF, Staufer U. Sensing protein molecules using nanofabricated pores. *Appl Phys Lett*. 2006; 88:093901.
83. Fologea D, Ledden B, McNabb DS, Li J. Electrical characterization of protein molecules by a solid-state nanopore. *Appl Phys Lett*. 2007; 91:38991.
84. Sexton LT, Horne LP, Sherrill SA, Bishop GW, Baker LA, Martin CR. Resistive-pulse studies of proteins and protein/antibody complexes using a conical nanotube sensor. *J Am Chem Soc*. 2007; 129:13144–13152. [PubMed: 17918938]
85. Han A, Creus M, Schurmann G, Linder V, Ward TR, de Rooij NF, Staufer U. Label-free detection of single protein molecules and protein-protein interactions using synthetic nanopores. *Anal Chem*. 2008; 80:4651–4658. [PubMed: 18470996]

86. Pedone D, Firnkjes M, Rant U. Data analysis of translocation events in nanopore experiments. *Anal Chem.* 2009; 81:9689–9694. [PubMed: 19877660]
87. Niedzwiecki DJ, Grazul J, Movileanu L. Single-molecule observation of protein adsorption onto an inorganic surface. *J Am Chem Soc.* 2010; 132:10816–10822. [PubMed: 20681715]
88. Firnkjes M, Pedone D, Knezevic J, Doblinger M, Rant U. Electrically Facilitated Translocations of Proteins through Silicon Nitride Nanopores: Conjoint and Competitive Action of Diffusion, Electrophoresis, and Electroosmosis. *Nano Lett.* 2010; 10:2162–2167. [PubMed: 20438117]
89. Sexton LT, Mukaibo H, Katira P, Hess H, Sherrill SA, Horne LP, Martin CR. An adsorption-based model for pulse duration in resistive-pulse protein sensing. *J Am Chem Soc.* 2010; 132:6755–6763. [PubMed: 20411939]
90. Freedman KJ, Jurgens M, Prabhu A, Ahn CW, Jemth P, Edel JB, Kim MJ. Chemical, Thermal, and Electric Field Induced Unfolding of Single Protein Molecules Studied Using Nanopores. *Anal Chem.* 2011; 83:5137–5144. [PubMed: 21598904]
91. Yusko EC, Johnson JM, Majd S, Prangko P, Rollings RC, Li J, Yang J, Mayer M. Controlling protein translocation through nanopores with bio-inspired fluid walls. *Nat Nanotechnol.* 2011; 6:253–260. [PubMed: 21336266]
92. Wei R, Gatterdam V, Wieneke R, Tampe R, Rant U. Stochastic sensing of proteins with receptor-modified solid-state nanopores. *Nat Nanotechnol.* 2012; 7:257–263. [PubMed: 22406921]
93. Nelson EM, Kurz V, Shim J, Timp W, Timp G. Using a nanopore for single molecule detection and single cell transfection. *Analyst.* 2012; 137:3020–3027. [PubMed: 22645737]
94. Cheley S, Xie H, Bayley H. A genetically encoded pore for the stochastic detection of a protein kinase. *Chembiochem.* 2006; 7:1923–1927. [PubMed: 17068836]
95. Xie H, Braha O, Gu LQ, Cheley S, Bayley H. Single-Molecule Observation of the Catalytic Subunit of cAMP-Dependent Protein Kinase Binding to an Inhibitor Peptide. *Chem Biol.* 2005; 12:109–120. [PubMed: 15664520]
96. Zhao Q, de Zoysa RS, Wang D, Jayawardhana DA, Guan X. Real-time monitoring of peptide cleavage using a nanopore probe. *J Am Chem Soc.* 2009; 131:6324–6325. [PubMed: 19368382]
97. Kukwikila M, Howorka S. Electrically sensing protease activity with nanopores. *J Phys Condens Matter.* 2010; 22:454103. [PubMed: 21339591]
98. Mohammad MM, Howard KR, Movileanu L. Redesign of a plugged beta-barrel membrane protein. *J Biol Chem.* 2011; 286:8000–8013. [PubMed: 21189254]
99. Mohammad MM, Iyer R, Howard KR, McPike MP, Borer PN, Movileanu L. Engineering a Rigid Protein Tunnel for Biomolecular Detection. *J Am Chem Soc.* 2012; 134:9521–9531. [PubMed: 22577864]
100. Howorka S, Movileanu L, Lu XF, Magnon M, Cheley S, Braha O, Bayley H. A protein pore with a single polymer chain tethered within the lumen. *J Am Chem Soc.* 2000; 122:2411–2416.
101. Movileanu L, Howorka S, Braha O, Bayley H. Detecting protein analytes that modulate transmembrane movement of a polymer chain within a single protein pore. *Nat Biotechnol.* 2000; 18:1091–1095. [PubMed: 11017049]
102. Howorka S, Nam J, Bayley H, Kahne D. Stochastic detection of monovalent and bivalent protein-ligand interactions. *Angew Chem Int Ed Engl.* 2004; 43:842–846. [PubMed: 14767954]
103. Rotem D, Jayasinghe L, Salichou M, Bayley H. Protein Detection by Nanopores Equipped with Aptamers. *J Am Chem Soc.* 2012; 134:2781–2787. [PubMed: 22229655]
104. Howorka S, Movileanu L, Braha O, Bayley H. Kinetics of duplex formation for individual DNA strands within a single protein nanopore. *Proc Natl Acad Sci U S A.* 2001; 98:12996–13001. [PubMed: 11606775]
105. Mayer M, Semetey V, Gitlin I, Yang J, Whitesides GM. Using ion channel-forming peptides to quantify protein-ligand interactions. *J Am Chem Soc.* 2008; 130:1453–1465. [PubMed: 18179217]
106. Astier Y, Kainov DE, Bayley H, Tuma R, Howorka S. Stochastic Detection of Motor Protein-RNA Complexes by Single-Channel Current Recording. *Chemphyschem.* 2007; 8:2189–2194. [PubMed: 17886244]

107. Hornblower B, Coombs A, Whitaker RD, Kolomeisky A, Picone SJ, Meller A, Akeson M. Single-molecule analysis of DNA-protein complexes using nanopores. *Nat Methods*. 2007; 4:315–317. [PubMed: 17339846]
108. Zhao Q, Sigalov G, Dimitrov V, Dorvel B, Mirsaidov U, Sligar S, Aksimentiev A, Timp G. Detecting SNPs using a synthetic nanopore. *Nano Lett*. 2007; 7:1680–1685. [PubMed: 17500578]
109. Benner S, Chen RJ, Wilson NA, Abu-Shumays R, Hurt N, Lieberman KR, Deamer DW, Dunbar WB, Akeson M. Sequence-specific detection of individual DNA polymerase complexes in real time using a nanopore. *Nat Nanotechnol*. 2007; 2:718–724. [PubMed: 18654412]
110. Cockroft SL, Chu J, Amorin M, Ghadiri MR. A single-molecule nanopore device detects DNA polymerase activity with single-nucleotide resolution. *J Am Chem Soc*. 2008; 130:818–820. [PubMed: 18166054]
111. Wanunu, M.; Meller, A. Single-molecule analysis of nucleic acids and DNA-protein interactions. In: Selvin, PR.; Ha, T., editors. *Single-molecule techniques: a laboratory manual*. New York: Cold Spring Harbor Laboratory Press; 2008. p. 395–420.
112. Smeets RM, Kowalczyk SW, Hall AR, Dekker NH, Dekker C. Translocation of RecA-coated double-stranded DNA through solid-state nanopores. *Nano Lett*. 2009; 9:3089–3096. [PubMed: 19053490]
113. Dorvel B, Sigalov G, Zhao Q, Comer J, Dimitrov V, Mirsaidov U, Aksimentiev A, Timp G. Analyzing the forces binding a restriction endonuclease to DNA using a synthetic nanopore. *Nucleic Acids Res*. 2009; 37:4170–4179. [PubMed: 19433506]
114. Kowalczyk SW, Hall AR, Dekker C. Detection of Local Protein Structures along DNA Using Solid-State Nanopores. *Nano Lett*. 2009; 10:324–328. [PubMed: 19902919]
115. Spiering A, Getfert S, Sischka A, Reimann P, Anselmetti D. Nanopore translocation dynamics of a single DNA-bound protein. *Nano Lett*. 2011; 11:2978–2982. [PubMed: 21667921]
116. Lin J, Fabian M, Sonenberg N, Meller A. Nanopore detachment kinetics of poly(A) binding proteins from RNA molecules reveals the critical role of C-terminus interactions. *Biophys J*. 2012; 102:1427–1434. [PubMed: 22455926]
117. Shim JW, Gu LQ. Encapsulating a single g-quadruplex aptamer in a protein nanocavity. *J Phys Chem B*. 2008; 112:8354–8360. [PubMed: 18563930]
118. Shim JW, Tan Q, Gu LQ. Single-molecule detection of folding and unfolding of the G-quadruplex aptamer in a nanopore nanocavity. *Nucleic Acids Res*. 2009; 37:972–982. [PubMed: 19112078]
119. Ding S, Gao C, Gu LQ. Capturing Single Molecules of Immunoglobulin and Ricin with an Aptamer-Encoded Glass Nanopore. *Anal Chem*. 2009; 81:6649–6655. [PubMed: 19627120]
120. Soskine M, Biesemans A, Moeyaert B, Cheley S, Bayley H, Maglia G. An engineered ClyA nanopore detects folded target proteins by selective external association and pore entry. *Nano Lett*. 2012; 12:4895–4900. [PubMed: 22849517]
121. Scheuring S, Muller DJ, Stahlberg H, Engel HA, Engel A. Sampling the conformational space of membrane protein surfaces with the AFM. *Eur Biophys J Biophys Lett*. 2002; 31:172–178.
122. Neuman KC, Nagy A. Single-molecule force spectroscopy: optical tweezers, magnetic tweezers and atomic force microscopy. *Nat Methods*. 2008; 5:491–505. [PubMed: 18511917]
123. Weisel JW, Shuman H, Litvinov RI. Protein-protein unbinding induced by force: single-molecule studies. *Curr Opin Struct Biol*. 2003; 13:227–235. [PubMed: 12727517]
124. Barsegov V, Thirumalai D. Probing protein-protein interactions by dynamic force correlation spectroscopy. *Phys Rev Lett*. 2005; 95:168302. [PubMed: 16241846]
125. Dudko OK, Mathe J, Szabo A, Meller A, Hummer G. Extracting kinetics from single-molecule force spectroscopy: nanopore unzipping of DNA hairpins. *Biophys J*. 2007; 92:4188–4195. [PubMed: 17384066]
126. Tabard-Cossa V, Wiggin M, Trivedi D, Jetha NN, Dwyer JR, Marziali A. Single-molecule bonds characterized by solid-state nanopore force spectroscopy. *ACS Nano*. 2009; 3:3009–3014. [PubMed: 19751064]
127. Brewer LR, Bianco PR. Laminar flow cells for single-molecule studies of DNA-protein interactions. *Nat Methods*. 2008; 5:517–525. [PubMed: 18511919]

128. Schwarzenbacher M, Kaltenbrunner M, Brameshuber M, Hesch C, Paster W, Weghuber J, Heise B, Sonnleitner A, Stockinger H, Schutz GJ. Micropatterning for quantitative analysis of protein-protein interactions in living cells. *Nat Methods*. 2008; 5:1053–1060. [PubMed: 18997782]
129. Raicu V, Jansma DB, Miller RJ, Friesen JD. Protein interaction quantified in vivo by spectrally resolved fluorescence resonance energy transfer. *Biochem J*. 2005; 385:265–277. [PubMed: 15352875]
130. Roy R, Hohng S, Ha T. A practical guide to single-molecule FRET. *Nat Methods*. 2008; 5:507–516. [PubMed: 18511918]
131. Raicu V, Stoneman MR, Fung R, Melnichuk M, Jansma DB, Pisterzi LF, Rath S, Fox M, Wells JD. Determination of supramolecular structure and spatial distribution of protein complexes in living cells. *Nature Photon*. 2009; 3:107–113.
132. Lamichhane R, Solem A, Black W, Rueda D. Single-molecule FRET of protein-nucleic acid and protein-protein complexes: surface passivation and immobilization. *Methods*. 2010; 52:192–200. [PubMed: 20554047]
133. Pisterzi LF, Jansma DB, Georgiou J, Woodside MJ, Chou JT, Angers S, Raicu V, Wells JW. Oligomeric size of the m2 muscarinic receptor in live cells as determined by quantitative fluorescence resonance energy transfer. *J Biol Chem*. 2010; 285:16723–16738. [PubMed: 20304928]
134. Albizu L, Cottet M, Kralikova M, Stoev S, Seyer R, Brabet I, Roux T, Bazin H, Bourrier E, Lamarque L, Breton C, Rives ML, Newman A, Javitch J, Trinquet E, Manning M, Pin JP, Mouillac B, Durroux T. Time-resolved FRET between GPCR ligands reveals oligomers in native tissues. *Nat Chem Biol*. 2010; 6:587–594. [PubMed: 20622858]
135. Padilla-Parra S, Tramier M. FRET microscopy in the living cell: different approaches, strengths and weaknesses. *Bioessays*. 2012; 34:369–376. [PubMed: 22415767]
136. Keyser UF, Koeleman BN, van Dorp S, Krapf D, Smeets RMM, Lemay SG, Dekker NH, Dekker C. Direct force measurements on DNA in a solid-state nanopore. *Nature Physics*. 2006; 2:473–477.
137. Keyser UF, van der DJ, Dekker C, Dekker NH. Inserting and manipulating DNA in a nanopore with optical tweezers. *Methods Mol Biol*. 2009; 544:95–112. [PubMed: 19488696]
138. Hall AR, Scott A, Rotem D, Mehta KK, Bayley H, Dekker C. Hybrid pore formation by directed insertion of alpha-haemolysin into solid-state nanopores. *Nat Nanotechnol*. 2010; 5:874–877. [PubMed: 21113160]
139. Rosenstein JK, Wanunu M, Merchant CA, Drndic M, Shepard KL. Integrated nanopore sensing platform with sub-microsecond temporal resolution. *Nat Methods*. 2012; 9:487–492. [PubMed: 22426489]

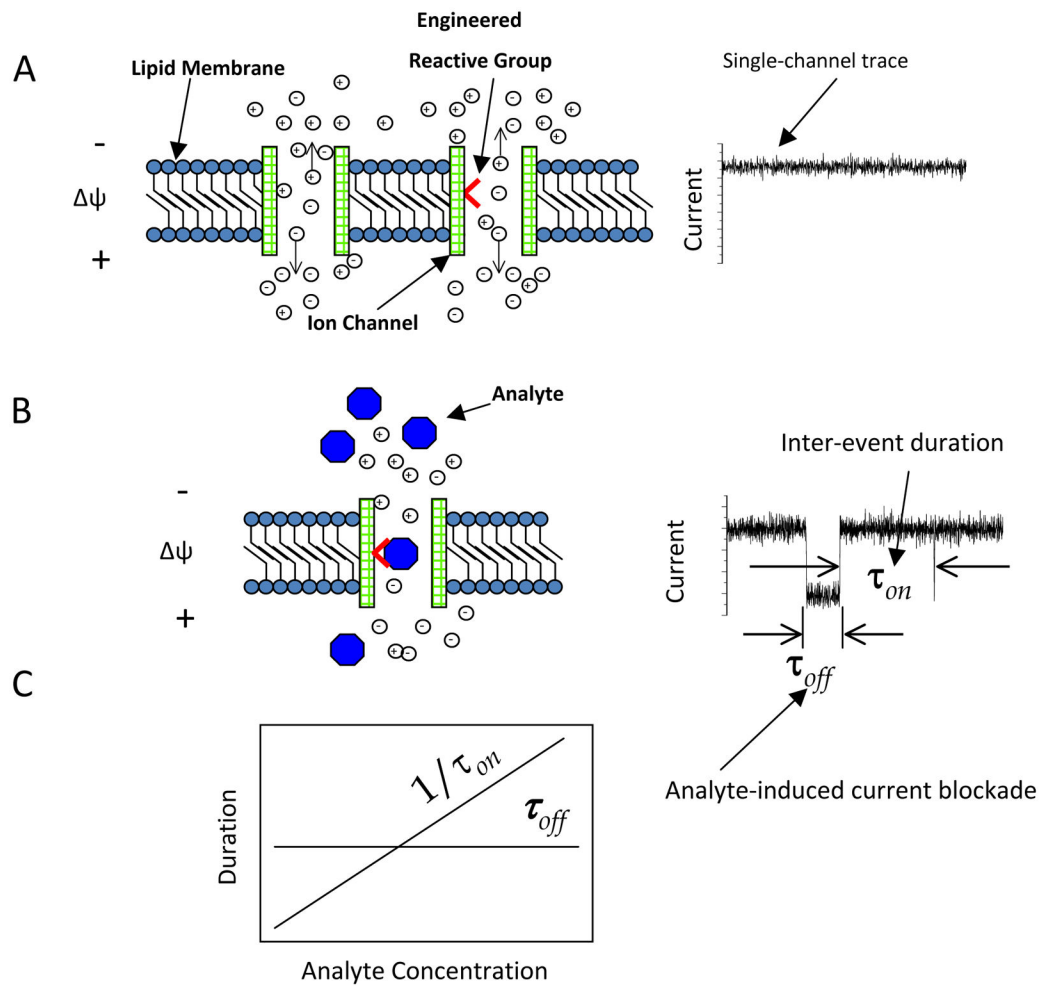


**Figure 1.**

The underlying mechanism of single-molecule detection using engineered protein nanopores. An open protein nanopore mediates the translocation of small ions through an insulating lipid bilayer. **(A)** If a transmembrane potential is applied, a single-channel electrical current is recorded owing to the passage of ions across the nanopore; **(B)** If both a transmembrane potential is applied and analytes are added to one of the chambers, non-covalently interactions of the analytes with the functional reactive group located within the pore lumen produce transient and reversible single-channel current blockades. These current depend on the strength of the interaction between analyte molecules and the reactive group; **(C)** The kinetics of non-covalent analyte-engineered reactive group interactions undergoes a bi-molecular kinetic scheme. Here, the time constant of dissociation,  $\tau_{off}$ , is independent of the analyte concentration. The rate constant of association,  $k_{on}$ , which is determined as  $1/(\tau_{on}c)$ , where  $\tau_{on}$  is the inter-event duration, and  $c$  is the concentration of analyte is proportional with the frequency of binding events. The rate constant of dissociation  $k_{off}$ , which is determined as  $1/\tau_{off}$ , where  $\tau_{off}$  is the event duration, is independent on the analyte concentration.  $\psi$  is the applied transmembrane potential. Direction of ion movements, which result from the application of an electrical force, is indicated by vertical arrows. Reproduced with permission from <sup>15</sup>.

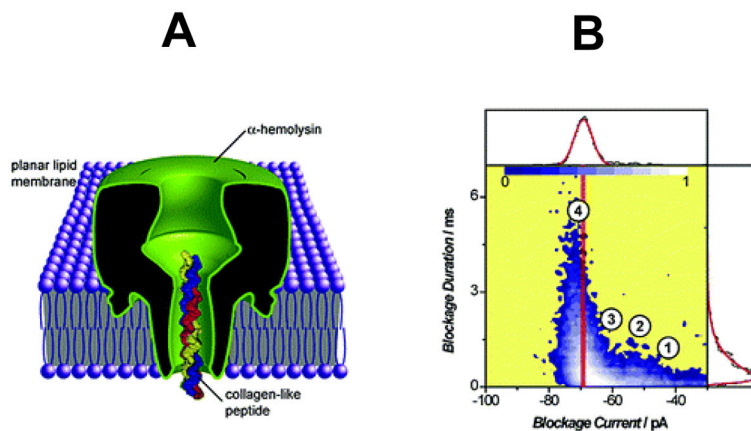


**Figure 2. Cartoon showing the  $\alpha$ -hemolysin ( $\alpha$ HL) protein nanopore inserted into a lipid bilayer (A) A cartoon that illustrates partitioning of a collagen-like polypeptide into the  $\beta$ -barrel domain of the interior of the  $\alpha$ HL protein nanopore. The inner diameter of the constriction of the nanopore is  $\sim 15$  Å; (B) A scatter plot representation of the single-channel current blockades observed with the  $\alpha$ HL protein nanopore in the presence of collagen-like polypeptides added to the chamber. Reproduced and adapted with permission from <sup>30</sup>.**

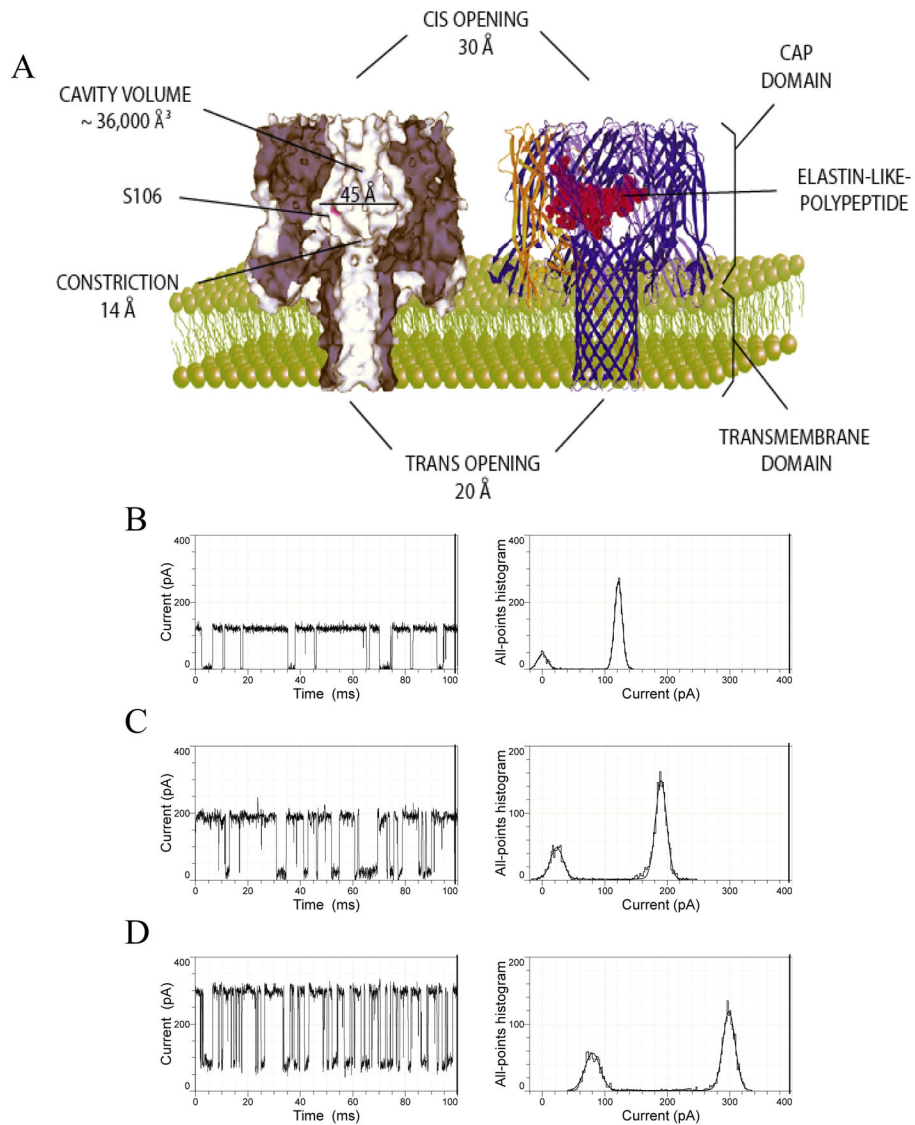


**Figure 3. Elastin-like polypeptide (ELP)-containing αHL protein is a temperature-responsive nanostructure**

(A) A cartoon showing the native and ELP loop-containing αHL protein nanopore; (B), (C) and (D) are single-channel electrical traces with an ELP loop-containing αHL protein nanopore recorded at 20, 40 and 60°C, respectively. The ELP loop contained 50 residues. Reproduced and adapted with permission from <sup>56</sup>.

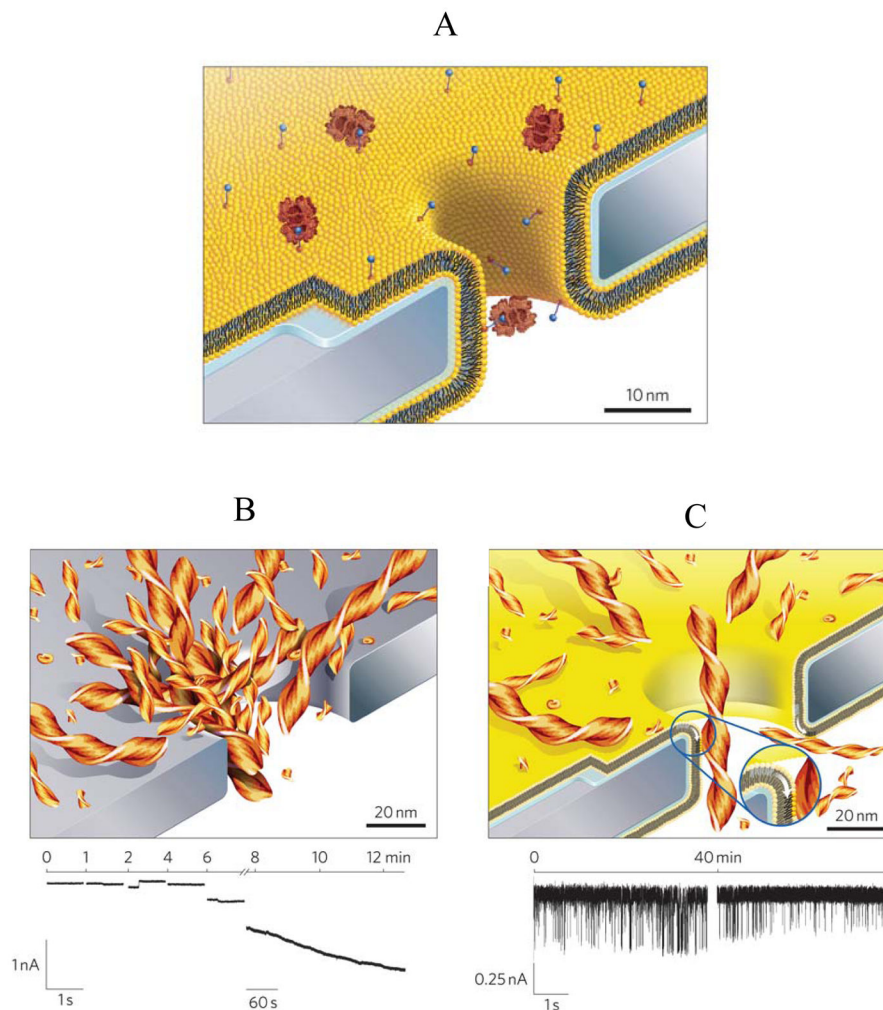


**Figure 4. Cartoon illustrating a new approach for protein translocation through a single solid-state nanopore in a silicon nitride membrane, which was coated with a fluid lipid bilayer** (A) Cartoon showing a lipid bilayer-coated, solid-state nanopore that incorporates biotin-containing lipids. Some biotin-containing lipids are bound to the interacting protein via specific ligand-protein interactions; (B) Cartoon and single-channel electrical trace indicating the clogging of an uncoated, solid-state nanopore with amyloid  $\beta$ -polypeptide ( $A\beta$ ) aggregates; (C) Cartoon and single-channel electrical trace indicating the absence of nonspecific protein adsorption and a representative single-channel trace including current blockades produced by the translocation of individual  $A\beta$  aggregates across a fluid lipid bilayer-coated, solid-state nanopore. Reproduced and adapted with permission from <sup>91</sup>.

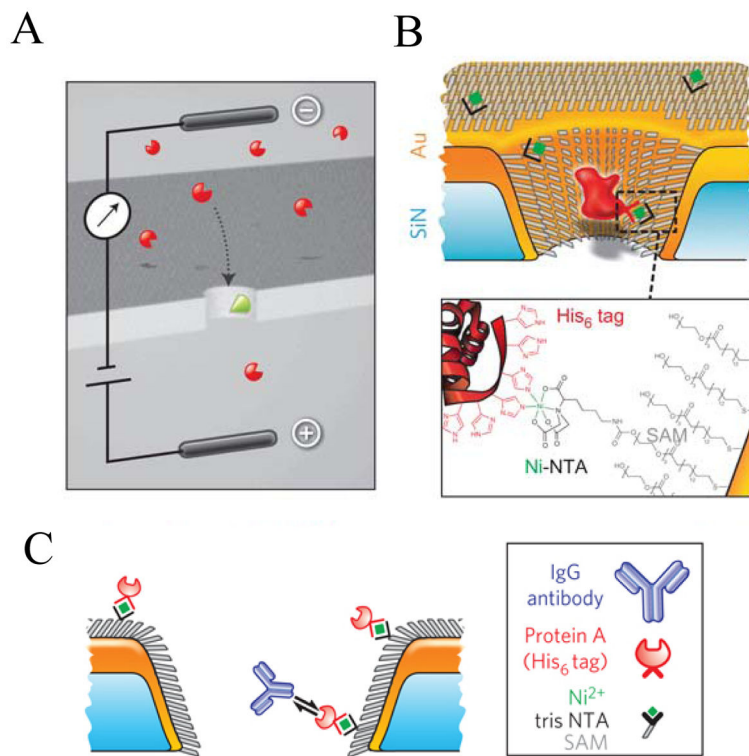


**Figure 5. Design of chemical functionalization of a metallized, solid-state nanopore for the single-molecule stochastic sensing of targeted proteins**

(A) Illustration of the voltage-clamp technique, in which single-channel current blockades are produced by the translocation of protein analytes; (B) Cartoon indicating the chemical functionalization of a metallized, solid-state nanopore with a single monolayer of alkane thiols (SAM), thiol-modified polyethylene glycol (PEG) chains as well as nitrilotriacetic (NTA) receptor thiols for binding to hexahistidine ( $\text{His}_6^+$ )-tagged receptor proteins; (C) Design of multiple modifications of a solid-state nanopore for capturing single proteins via protein-antibody interactions. The solid-state nanopore is modified first through thiol-containing SAM and PEG layers. His-tagged protein A is stably immobilized within a NTA-modified nanopore. Individual current blockades were recorded through interactions of IgG antibody to Protein A. Reproduced and adapted with permission from <sup>92</sup>.